MOLECULAR PHARMACOLOGY, 18, 167-178

Sites of Action of Phencyclidine

II. Interaction with the Ionic Channel of the Nicotinic Receptor

EDSON X. ALBUQUERQUE, MING-CHENG TSAI, ROBERT S. ARONSTAM,[1] AMIRA T. ELDEFRAWI AND MOHYEE E. ELDEFRAWI

Department of Pharmacology and Experimental Therapeutics, University of Maryland School of Medicine, Baltimore, Maryland 21201

Received October 9, 1979; Accepted March 20, 1980

SUMMARY

ALBUQUERQUE, E. X., M.-C. TSAI, R. S. ARONSTAM, A. T. ELDEFRAWI AND M. E. ELDEFRAWI. Sites of action of phenylcyclidine. II. Interaction with the ionic channel of the nicotinic receptor. *Mol. Pharmacol.* **18:** 167-178 (1980).

The effects of phencyclidine (PCP) were studied on the endplate current (EPC), miniature endplate current (MEPC), and synaptic noise of the frog sartorius muscle and on the binding of [^{3}H]perhydrohistrionicotoxin ([^{3}H]H_{12}-HTX) to the ionic channel of the acetylcholine (ACh) receptor in electric organ membranes of *Torpedo ocellata*. PCP decreased the peak amplitude of the EPC in a voltage- and time-dependent manner, caused nonlinearity in the current-voltage relationship, accelerated the decay time constants of the EPC and MEPC, and shortened the mean lifetime of the single ionic channel. PCP also inhibited binding of [^{3}H]H_{12}-HTX to the ionic channel of the ACh receptor with a K_i of 6.9 μM. When carbamylcholine was present to activate the ACh receptors, the K_d value for PCP binding to ionic channel sites was reduced from 10.3 ± 4.2 to 2.0 ± 1.3 μM, thus showing higher affinity for the activated ionic channel sites. In addition, PCP also reacted with the closed ionic channel since a time-dependent effect on EPC amplitude in hyperpolarized membranes was observed even before the ACh receptor was activated. Further, PCP depressed peak EPC amplitude more markedly than it shortened the EPC decay time constant, thus disclosing that the depression of the former cannot be accounted for totally by the action of the agent on the open conformation of the ionic channel. A hybrid model was proposed to account for the interactions of PCP with the open and closed states of the ionic channel of the ACh receptor. The actions of PCP on both states of the ionic channel are qualitatively similar to those seen with histrionicotoxin.

INTRODUCTION

Phencyclidine (PCP)[2] and several of its derivatives have been shown to possess anticholinergic activity in a variety of nicotinic synapses, including frog muscles (1, 2, 3). Very recently, we have demonstrated that PCP was unable to protect against the binding of ACh or α-bungarotoxin (α-BGT) but significantly affected the endplate current (EPC) by blocking the conductance of the ionic channel and inhibiting the binding of perhydrohistrionicotoxin (H_{12}-HTX) (4). Another laboratory also observed that PCP at concentrations which blocked the response of the rectus abdominis frog muscle to ACh, did not block α-BGT binding (5).

Applying biophysical and biochemical techniques we can now distinguish drugs that interact with the ACh-receptor sites from ones that interact with its ionic channel sites. In fact, not only do these sites differ in their drug specificity, but they also differ in the characteristics of their interactions. Indeed, while the receptor sites bind ACh, α-BGT (6), and nereistoxin (7) in a voltage-independent manner, the channel sites react with histrionicotoxin (HTX) or its saturated analog H_{12}-HTX (8, 9), and amantadine (10), in a voltage-dependent manner. Drugs that interact with the ionic channel sites affect the

This study was supported in part by grants from the National Institutes of Health (NS-12063 to E.X.A. and NS-15261 to A.T.E.) and by Army Research Office Grant DAAG 29-78-G-0203 to M.E.E. and E.X.A.

[1] Present address: Department of Pharmacology, Medical College of Georgia, Augusta, Ga. 30912.

[2] Abbreviations used: PCP, phencyclidine; ACh, acetylcholine; HTX, histrionicotoxin; H_{12}-HTX, perhydrohistrionicotoxin; α-BGT, α-bungarotoxin; EPC, endplate current; MEPC, miniature endplate current.

0026-895X/80/050167-12$02.00/0

time course of the EPC, render the current–voltage relationship nonlinear, and compete with HTX for binding to these sites (10). On the other hand, there are drugs that interact with both kinds of sites at rather similar concentrations, such as quinacrine (11), piperocaine (12), and tetraethylammonium (13).

In the previous paper (14), we showed that PCP inhibited the extrajunctional ACh sensitivity of denervated muscle, and concluded that PCP reacted with the ACh receptor–ionic channel complex. However, since PCP did not inhibit [^{3}H]ACh or [^{125}I]α-BGT binding to the ACh-receptor sites, nor did PCP protect muscle twitch or extrajunctional ACh sensitivity against blockade by α-BGT, we suggested that the PCP effect had to be due to its binding to the ionic channel of the ACh receptor. The present investigation was initiated to determine if indeed PCP interacts with the ionic channel of the ACh receptor. We utilized biophysical and biochemical techniques for the study, the first for investigations of EPCs and ACh noise analyses. Using biochemical methods, we studied the effect of PCP on binding of [^{3}H]H_{12}-HTX to the ionic channel in a tissue that is rich in nicotinic ACh receptors, namely, the electric organ of the electric ray, *Torpedo ocellata*.

MATERIALS AND METHODS

Electrophysiological techniques. The conditions and solutions used in electrophysiological measurements of frog endplates were as described in the previous paper (14).

For intracellular recordings the voltage clamp circuitry was similar to that described previously (12, 13). Glass microelectrodes filled with 3 M KCl and having resistances of 2–8 MΩ were used for recording and passing current. To investigate the voltage- and time-dependent changes of the EPC induced by PCP, conditioning steps of varied duration were used (14). Voltage sequence A was similar to that previously used for examining HTX-treated fibers (15, 16). This voltage sequence was made up of successive 3-s-long, 10-mV steps starting from a holding potential of −50 mV. The conditioning steps were made sequentially in the depolarizing and then the hyperpolarizing direction between the voltage extremes of +80 and −180 mV. After the periodic generation of an EPC, the conditioning potential was manually stepped with a decade potentiometer to a new level. A 3-s conditioning step (voltage sequence A) was used because it was previously shown that when fibers were exposed to 35 μM HTX, EPC amplitudes attenuated rapidly when they were generated at a high frequency such as 20 Hz (17). Furthermore, long steps minimized to a certain degree the error in the manually controlled conditioning duration.

Voltage sequence B was used to test the influence of conditioning step length on the relationship between EPC and the membrane potential. This sequence required that the endplate be clamped for periods ranging from 25 ms to 5 s at a particular level before the EPC was elicited. The pulses were presented consecutively in the depolarizing and then the hyperpolarizing direction as they were in voltage sequence A. EPCs were evoked automatically 5–10 ms before the end of the conditioning pulse. EPCs were sampled, digitized, and analyzed with the aid of a PDP11/40 computer.

To record and analyze the EPC fluctuations in response to iontophoretic application of ACh (ACh noise analysis), techniques similar to those described previously (13) were used. To deliver ACh, micropipets were used which would pass positive currents and which would have no leakage of ACh when a small negative braking current (<15 nA) was applied. Microelectrodes were selected for these characteristics using chronically denervated (7–10 days) rat soleus muscles mounted beside the experimental muscle in the tissue bath. The distance of the pipet from the muscle was approximately 25–50 μm, and ACh was released for 20–30 s. Iontophoretic currents were displayed on a Mingograf 81 polygraph having a frequency response from dc to 500 Hz, and recorded on a four-channel Tandberg FM tape recorder. A low-gain dc trace was used to measure the mean iontophoretic current during iontophoresis of ACh, while the high-gain ac coupled trace was used for the EPC fluctuation analysis. The sampling rate for the PDP11/40 computer was 2 kHz, and the signal was filtered (Krohn-Hite 3700 bandpass filter) between 1 and 800 Hz. For the ACh noise spectra the FFT (Fast Fourier transform) was applied to 512-point segments prior to and during application of 5- to 75-nA currents of ACh. Data segments were examined to exclude from the analysis any noise segments that contained miniature endplate currents (MEPCs). For the MEPC spectra, cells displaying a high MEPC frequency were used; the average spectrum of the baseline noise of the cell was subtracted from that obtained from several segments containing one to three MEPCs each. Spectra of ACh noise and of MEPCs were fitted by the least-squares method to a single Lorentzian curve for computation of single-channel conductance (γ) (ACh noise spectra only) and channel lifetime (τ_I) according to the formula $\tau_I = 1/(2\pi fc)$, where fc is the half-power frequency of the Lorentzian curve. Channel conductance was obtained from the ACh noise spectra ($\gamma_S = S(0)/4\mu_I(V - V_{eq})\tau_I$) or from variance of current noise using the formula $\gamma_V = \sigma_I^2/\mu_I(V - V_{eq})$ (15, 20).

Biochemical techniques. The membrane preparation from *Torpedo* electric organ is the same as described in the previous paper. [^{3}H]H_{12}-HTX (sp act 21 Ci/mmol) was obtained by tritiation of isodihydrohistrionicotoxin and its activity tested on frog sartorius muscle as described (9). Binding was determined by a filtration assay where a membrane preparation (50 μg protein) was incubated for 30 min at 22°C in 50 mM Tris–HCl, pH 7.4, and [^{3}H]H_{12}-HTX at the required concentration in a final volume of 1 ml. The mixture was filtered on Whatman GF/B glass fiber filters, and the filters were rinsed once with 7 ml of the Tris buffer. Each filter was placed in a 10-ml Filmware bag (Nalge/Sybron), 5 ml of toluene scintillation solution was added, and after 10 h the radioactivity was counted in a Beckman 3133 P liquid scintillation spectrometer. Since quinacrine inhibited competitively [^{3}H]H_{12}-HTX binding to ionic channel sites in *Torpedo* membranes (11), nonspecific binding was determined by including 0.1 mM quinacrine in a duplicate

series of incubation media as previously described (18). The interaction of PCP with the ion channel was determined from its inhibition of specific [^{3}H]H_{12}-HTX binding. The concentration of [^{3}H]H_{12}-HTX used was only a small fraction of its ion channel dissociation constant (100–300 nM), and less than 0.1% of the channels were complexed with [^{3}H]H_{12}-HTX. The concentrations of free ligands ([^{3}H]H_{12}-HTX and PCP) were adjusted by the amount of ligands that were bound. The inhibition constant (K_i) was determined from the slopes of double-reciprocal plots of [^{3}H]H_{12}-HTX binding curves performed in the presence of various concentrations of PCP. The dissociation constant (K_d) was determined from Scatchard plots of the occupancy by PCP of the ionic channel binding site as inferred from its inhibition of specific [^{3}H]H_{12}-HTX binding. Although determined by different procedures, K_i and K_d are both measures of PCP affinity for the ionic channel and should agree.

RESULTS

Effect of PCP on the voltage dependence of the peak EPC amplitude. PCP at concentrations ranging from 3 to 100 μM caused a significant decrease in the peak amplitude of the EPC and induced a marked nonlinearity in the current-voltage relationship (Table 1). Figure 1 shows families of EPCs in control muscles and after the addition of 60 μM PCP. In the presence of PCP, EPC amplitudes were depressed at all membrane potentials. However, the depression was not uniform but increased progressively with membrane hyperpolarization. This led to nonlinear current-voltage relationships as shown in Fig. 2 for several PCP concentrations. The minimum effective concentration for altering the EPC amplitude was 3 μM, which had little effect between +50 and −50 mV, but reduced the EPC amplitude significantly between −100 and −150 mV. With PCP at concentrations of 10, 30, and 60 μM, the EPC amplitude was depressed even at positive membrane potentials. At negative potentials, the EPC amplitudes showed a marked upward

TABLE 1

Effects of various concentrations of PCP on the rise time, amplitude, and the time constant of EPC decay on frog sartorius muscle held at −90 mV

Condition	Amplitude (× 10^{-7} A)	Rise time (ms)	Time constant of EPC decay (ms)
Control	4.56 ± 0.37 (14)[a]	0.78 ± 0.03	1.67 ± 0.04
PCP (1 μM)	4.07 ± 0.31 (17)	0.76 ± 0.04	1.66 ± 0.04
PCP (3 μM)	3.36 ± 0.27 (4)	0.75 ± 0.04	1.56 ± 0.06
PCP (10 μM)	2.53 ± 0.41 (14)[b]	0.69 ± 0.02[c]	1.42 ± 0.05[d]
PCP (30 μM)	1.02 ± 0.19 (15)[b]	0.62 ± 0.01[d]	0.95 ± 0.04[b]
PCP (60 μM)	0.46 ± 0.10 (8)[b]	0.56 ± 0.05[d]	0.63 ± 0.02[b]
PCP (100 μM)	0.40 ± 0.09 (6)[b]	0.52 ± 0.07[d]	0.54 ± 0.02[b]
Washing[e]	3.96 ± 0.20 (10)[c]	0.81 ± 0.04	1.48 ± 0.07

[a] The values in parentheses refer to the number of surface fibers sampled.

[b] Differ significantly from control ($P < 0.05$).

[c] Differ significantly from control ($P < 0.01$).

[d] Differ significantly from control ($P < 0.001$).

[e] Values refer only to muscles previously exposed to 30 μM PCP for 60 to 120 min.

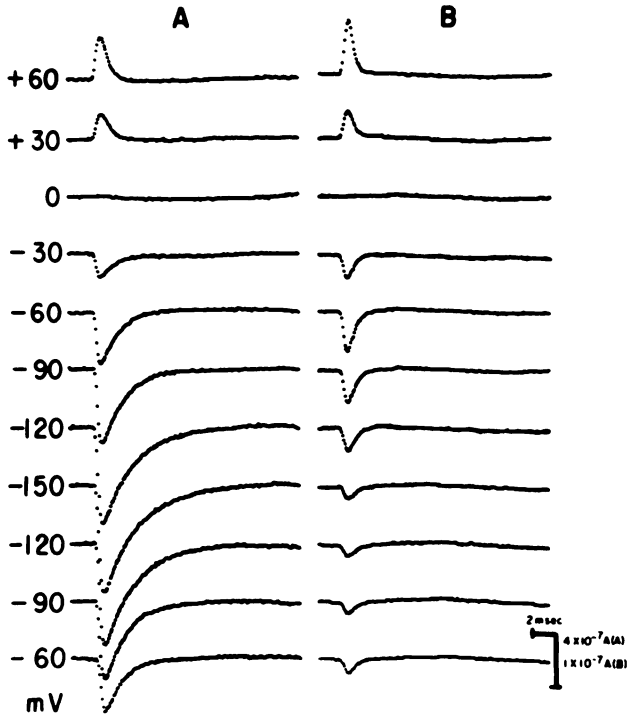

FIG. 1. *Digitized computer output of EPCs at various membrane potentials from (−150 to +60 mV) after 30–60 min exposure to PCP (30 μM) using 3-ms conditioning steps in the form of voltage sequence A*

The sequence of steps began at a holding potential of −60 mV and progressed first toward positive values, returning to very negative values, and finally terminating at −60 mV using 10-mV steps.

curvature, and a region of negative conductance where the EPC amplitudes actually decreased in spite of increases in driving force. These actions of PCP were slowly reversible such that after 2 h of continuous washing of the muscles with normal Ringer's solution the EPC peak amplitude recovered to 70% of its control value.

The onset of nonlinearity in the current-voltage relationship was shifted to more depolarized membrane potentials as the concentration of PCP was increased. In the presence of 3 μM PCP the nonlinearity started to occur at −64 mV, while at concentrations of 10, 30, and 60 μM the nonlinear segment began at about −48, −32, and −18 mV, respectively (Fig. 2, inset).

The time-dependent effect of PCP on the peak amplitude of the EPC. In the presence of PCP the slope of the current-voltage relationship became highly dependent upon membrane potential as the direction of the membrane potential was changed, such that a loop was formed. This nonlinearity was obtained using conditioning pulses of 3 s (voltage sequence A) and changes in membrane potential in the hyperpolarizing and then depolarizing direction, suggesting a combined voltage- and time-dependent effect of PCP on the EPC. Thus, with 3-s conditioning pulse durations, the EPC amplitude in most cells was larger during the initial hyperpolarizing steps from −50 to −150 mV than it was at the corresponding potentials on the return excursion from −150 to −50 mV. This led to a "hysteresis" loop which resembled that observed with HTX (15–17). In the majority of the endplates studied, hysteresis was detected at PCP con-

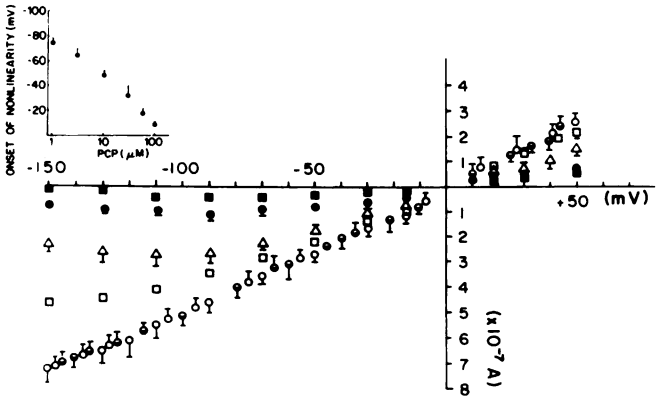

FIG. 2. *Current-voltage relationships of the EPC peak amplitude recorded under control condition using alternatively voltage sequence A* (○) *and voltage sequence B (pulse duration 25 ms)* (◒) *and in presence of PCP for 60–120 min: 3 μM* (□); *10 μM* (△); *30 μM* (●); *60 μM* (■)

The inset illustrates the relationship between PCP concentration and the onset of nonlinearity in the current-voltage relationship. The point at which the EPC amplitude departed from linearity was measured from the straight-line fit along the positive to negative potentials. The progressive increase in the concentration caused a deviation of the onset of nonlinearity to less negative membrane potentials. Each point is the mean ± SEM for 10 measurements in at least five muscles/concentration of drug used. When no bar is shown the SEM is inside the point.

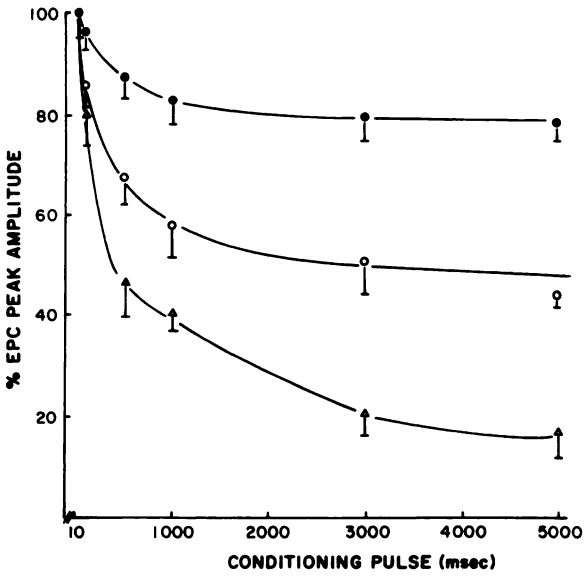

FIG. 4. *The effect of conditioning durations (voltage sequence B) on percentage peak amplitude of EPC at various holding potentials: −75 to −80 mV* (●); *−100 to −110 mV* (○); *and −150 to −160 mV* (△) *in the presence of PCP (30 μM)*

Each symbol and vertical bar represents mean ± SEM in six experiments.

centrations from 3 to 60 μM (Figs. 1 and 3A). To obtain these curves, the membrane was first clamped to −50 mV and then shifted sequentially in 10-mV steps to positive values (up to +80 mV) (arrow 1 in Fig. 3A), then toward negative potentials (arrows 2 and 3), and finally terminating at −50 mV (arrow 4). The membrane was held at the indicated potentials for approximately 2.5 s. The hysteresis loop was quite prominent in 10 μM PCP, but somewhat less conspicuous in 60 μM PCP. When the current-voltage relationship was studied using conditioning pulses of 25-ms duration (sequence B), a linear relationship was obtained regardless of the direction of the voltage steps at either PCP concentration (Fig. 3B). Although linear, the current-voltage plots with sequence B had a reduced slope conductance relative to control which resembled values on the linear portion of curves obtained using the initial hyperpolarizing excursion of

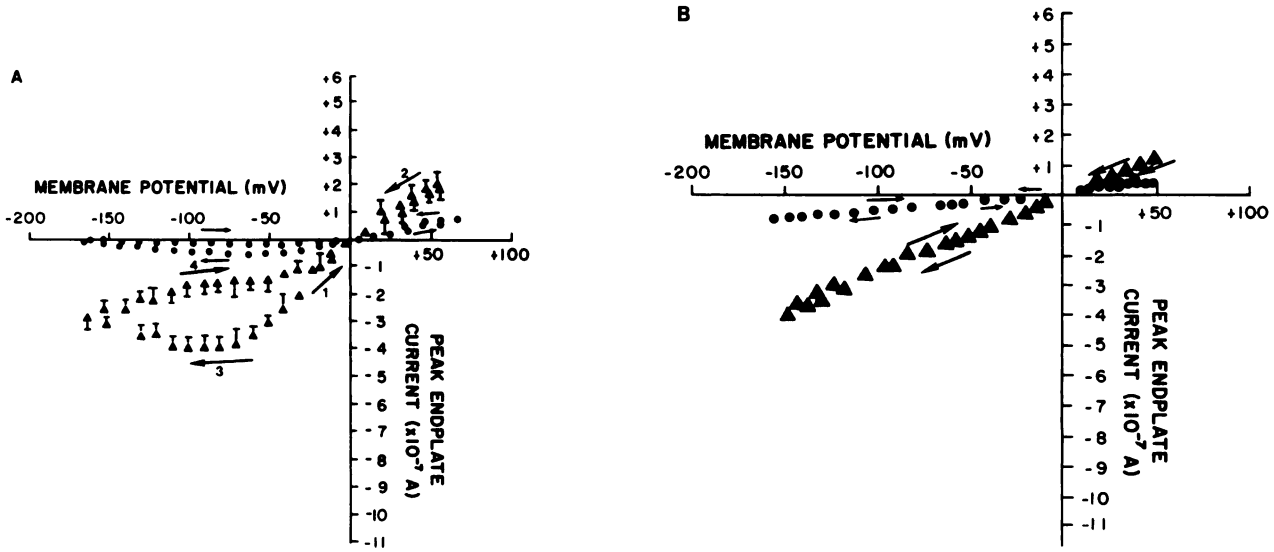

FIG. 3. *The effect of PCP on the current-voltage relationship of the peak amplitude of EPC using conditioning steps of 3 s (voltage sequence A) for A and 25 ms (voltage sequence B) for B*

The concentrations of PCP for both A and B were 30 μM (▲) and 60 μM (●), and the recordings were made after 30–60 min of exposure to PCP. The sequence of conditioning steps was initiated at a clamped holding potential of −50 mV and advanced first to positive potentials (arrow 1) and then to negative potentials following the direction of the arrows (2 and 3) and terminating at −50 mV (arrow 4). Although significant nonlinearity and looping were observed in A, linearity was however achieved in B when a 25-ms conditioning pulse was used.

sequence A (Fig. 2). The control current–voltage plots were essentially identical with either sequence A or B (Fig. 1). Since both the nonlinearity and hysteresis vanished with brief conditioning durations, it appeared that both were caused by a similar process. The process leading to a voltage-pathway sensitivity required a conditioning pulse longer than 25-ms duration.

To determine the precise time dependence of PCP's action, the membrane potential was stepped from the holding potential of −50 mV to −75, −100, or −150 mV. The nerve was stimulated with varied latencies such that the EPCs occurred after conditioning pulses of 25, 100, 500, 3000, and 5000 ms (Fig. 4). When the membrane was stepped from −50 to more hyperpolarized levels, the EPC amplitudes decreased along an approximately exponential path, reaching 80% of the initial amplitude at −75 mV, 50% at −100 mV, and 20% at −150 mV. The rate of equilibration to the test potentials was 1.6, 3, and 5 sec^{-1}, respectively, at the three test potentials. This finding indicated that the voltage- and time-dependent depression of the peak EPC amplitude induced by PCP was increased as the membrane was hyperpolarized. The long relaxation times following perturbations in the membrane potential indicated the presence of a very slow reequilibration of the drug-bound channels or a very slow conformational change.

The voltage-dependent effect of PCP on the EPC amplitude did not require previous activation of the ACh receptor. The membrane potential was clamped at −50 mV and the EPC recorded; then the membrane potential was stepped to −150 mV and held there for 30 s. Finally, the membrane potential was returned to −50 mV and the EPC recorded immediately (within 20 ms). In the presence of PCP (60 μM), the peak EPC amplitude after the step was depressed to 18 ± 6.9% (n = 12) of its value prior to the step. Thus, the site of action of PCP appeared to be available in the absence of ACh, implicating the closed or resting conformation of the ACh receptor–ionic channel complex as the molecular target.

It was possible that the long clamp durations used to disclose the marked voltage- and time-dependent effects might be due to major perturbations of the lipid arrangement of the membrane which would influence time-dependent shifts in ion concentrations during generation of the EPC. However, the use of different conditioning pulses, as brief as 25 ms and as long as 3 s for the evaluation of the null potential, revealed no significant changes from control condition during exposure to 30 and 60 μM PCP (Table 2). Thus, these studies disclosed that PCP did not affect the ion concentration shifts (Table 2) during its reaction with the ionic channel in either closed or open conformation.

Acceleration of the time constant of decay induced by PCP. Simultaneously with the marked depression of the EPC peak amplitude, PCP caused acceleration of both the rise time and decay time constant of the EPC (τ_{EPC}) (Table 1). Indeed, at concentrations ranging from 10 to 100 μM, PCP caused significant shortening of the decay phase of the EPC (Figs. 5 and 6). The EPC decay recorded at three membrane potentials of +50, −90, and −150 mV remained a single exponential function of time over most of its decay phase during control condition and after exposure for 120 min to PCP at all concentrations studied. However, PCP caused marked alteration in the time constant EPC decay and its dependence on membrane potential (Fig. 5). For example, the EPC decay at −150 mV was 8.3 ms in control condition (obtained at the intercept of the decay phase at 10% of peak amplitude and the abscissa), while in 10 and 30 μM PCP they were 6.1 and 2.8 ms, respectively. At +60 mV these concentrations of PCP had little or no effect on the EPC decay. The PCP-induced alteration of the voltage dependence of τ_{EPC} is shown in Fig. 6 for a range of five different concentrations of PCP.

A relationship exists between peak EPC amplitude and τ_{EPC} such that a decrease in τ_{EPC} could lead to reduction in the EPC amplitude. In the present analysis the effect of PCP on the peak amplitude of the EPC was dependent upon the conditioning pulse while the effect on τ_{EPC} remained the same regardless of the conditioning pulse used. These findings support the notion that the change in τ_{EPC} cannot explain the voltage- and time-dependent decrease in EPC amplitude. Further, the concentrations of PCP that caused alteration in the peak amplitude of

TABLE 2

Action of PCP on the EPC null potential (mV)[a]

Condition	N[b]	Duration of conditioning pulse	
		20 ms	3 s
Control	20	+1.34 ± 0.06	+1.73 ± 0.04
PCP (1 μM)	12	−1.98 ± 0.07	+1.41 ± 0.03
PCP (3 μM)	10	+0.93 ± 0.06	+1.33 ± 0.01
PCP (10 μM)	17	+1.13 ± 0.07	+0.68 ± 0.14
PCP (30 μM)	13	+0.93 ± 0.04	+0.91 ± 0.09
PCP (60 μM)	19	+0.97 ± 0.09	+0.87 ± 0.07

[a] The values refer to 60–120 min after equilibration in the drug. Each value represents the mean ± SEM of four muscles.

[b] N, number of endplates tested per single muscle fiber.

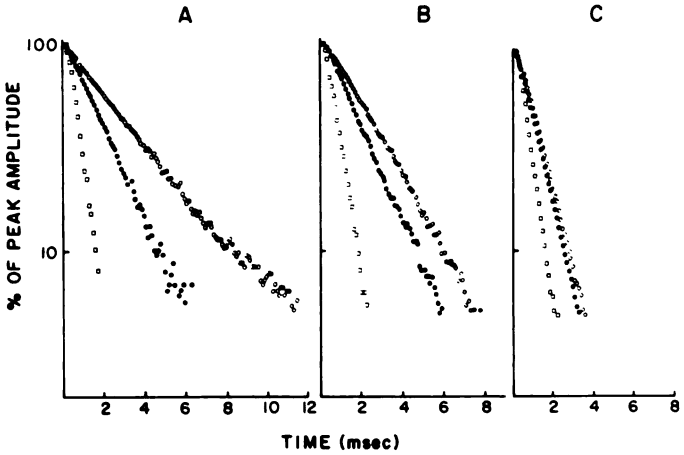

FIG. 5. *The effect of PCP on the decay phase of EPC recorded at three holding potentials*

(A) Control conditions; (B and C) in presence of 10 and 30 μM PCP, respectively. Recordings at −150 mV (○); −90 mV (●); +60 mV (□). Note the marked acceleration of the decay phase and no change in the single exponential nature of the decay.

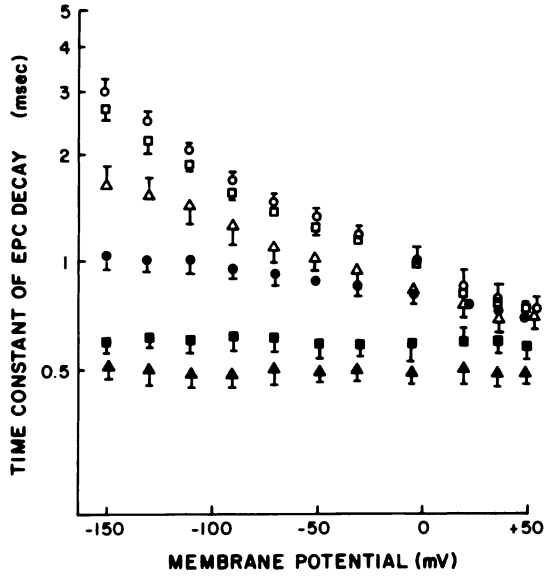

FIG. 6. *Semilogarithmic plots illustrating the relationship between the time constant of EPC decay and membrane potential in control* (○) *and during exposure to various concentrations of PCP: 3 μM* (□); *10 μM* (△); *30 μM* (●); *60 μM* (■); *and 100 μM* (▲)

Each symbol and vertical bar is the mean ± SEM of 5–10 fibers in three muscles.

the EPC also induced an acceleration of the decay phase. However, the shortening of the decay phase and depression of the peak amplitude were altered to different extents by the same concentrations of PCP (Fig. 7).

Effect of PCP on the MEPCs and on the elementary conductance. To determine whether γ and τ_I underlie the effects of PCP on the EPC, studies were made of the decay phase and peak amplitude of the MEPC and of τ_I as determined from analysis of ACh noise spectra in the presence of several concentrations of the agent. Similar to its action on the EPC, PCP caused a significant reduction in the MEPC peak amplitude (Fig. 8A). For example, at a concentration of 30 μM, the amplitude of the MEPCs recorded at −90 mV was reduced by 91%.

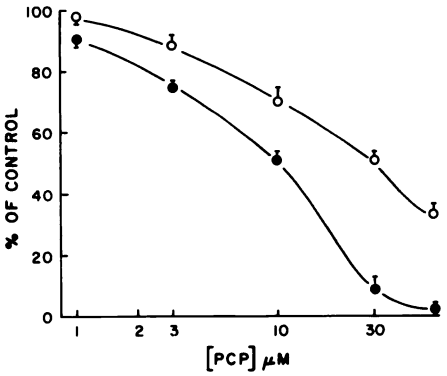

FIG. 7. *Dose-response relationships accompanying the effect of PCP on the peak amplitude and time constant of the EPC decay*

The depression of the peak amplitude (●) during exposure to PCP for 60 min was more marked than the shortening of the time constant of EPC decay (○). Mean ± SEM from 10–15 fibers per concentration used from at least four muscles. Values sampled at holding membrane potential −90 mV.

Mean channel lifetime obtained from MEPC spectra and the τ of the MEPC (τ_{MEPC}) were shortened in the presence of PCP (Table 3). At −90 mV, τ_{MEPC} was reduced markedly from 2.2 ms in control condition to 1.14 and 0.78 ms in the presence of 10 and 30 μM PCP, respectively (Figs. 8C and D). Thus, τ_{MEPC} obtained by calculating the decay time constant or by spectral analysis of the MEPCs exhibited a marked change from voltage dependence to voltage independence in the presence of PCP, a change which corresponded to that seen in τ_{EPC}. Although PCP affected both peak amplitude and τ_{MEPC}, these two parameters displayed different concentration dependencies. The decay phase and depression of peak amplitude were indeed altered at different rates at the various concentrations of PCP used (Fig. 8B), suggesting that shortening of the lifetime of open endplate channels could not account for the marked depression of the MEPC amplitude.

If one assumes that the rate-limiting reaction during the decay phase of the MEPC reflects a conformational relaxation of the open ionic channel to its closed state, τ_{MEPC} must be equal to τ_I, and this similarity must be present at any given membrane potential. However, as shown in Table 3 and Figs. 8C and D and 9, it is obvious that τ_I was significantly shortened with respect to τ_{MEPC}. This phenomenon has also been observed on the sartorius muscle of *Rana temporaria* (20, 21) and the toad *Bufo marinus* (22). Several explanations have been put forward to explain this difference, but it is most likely related to the persistence of ACh in the synaptic cleft (20). PCP shortened both τ_{MEPC} and τ_I, and the difference between these two parameters in control was maintained in the presence of PCP.

PCP (3 μM) significantly depressed the EPC induced by iontophoresis of ACh to the junctional region (Fig. 9), but did not affect γ recorded at membrane potentials ranging from −50 to −120 mV. The values of γ remained similar to control at −90 mV (Table 3). The absence of changes in γ indicates that the decrease in MEPC and EPC amplitudes observed in the presence of PCP could not be explained by a decrease in the conductance of the channels opened by ACh, and thus a voltage-dependent shortening in channel lifetime and/or blockade of closed channels may be a more plausible explanation. In contrast to the lack of effect of PCP on γ, τ_I in the presence of PCP was shortened with respect to control. For example, as illustrated in Fig. 9B and Table 3, τ_I was shortened from 1.69 ms in control condition to 1.55 and 1.35 ms in the presence of 1 and 3 μM PCP, respectively. In making these studies of the EPC fluctuations in the presence of microiontophoretically applied ACh, it was necessary to use concentrations of PCP lower than those used to study the MEPCs and neurally evoked EPCs. Since PCP depressed so much the iontophoretically evoked EPC, concentrations greater than 3 μM did not allow a reliable spectral analysis. Some of this differential effect caused by PCP has been previously seen with toxins such as HTX and quinacrine (16).

Effect of PCP on binding of [^{3}H]H_{12}-HTX to the ionic channel of the ACh receptor. The quinacrine-sensitive binding of [^{3}H]H_{12}-HTX (2 nM) to *Torpedo* electric organ membranes was inhibited by PCP (Fig. 10). Double-

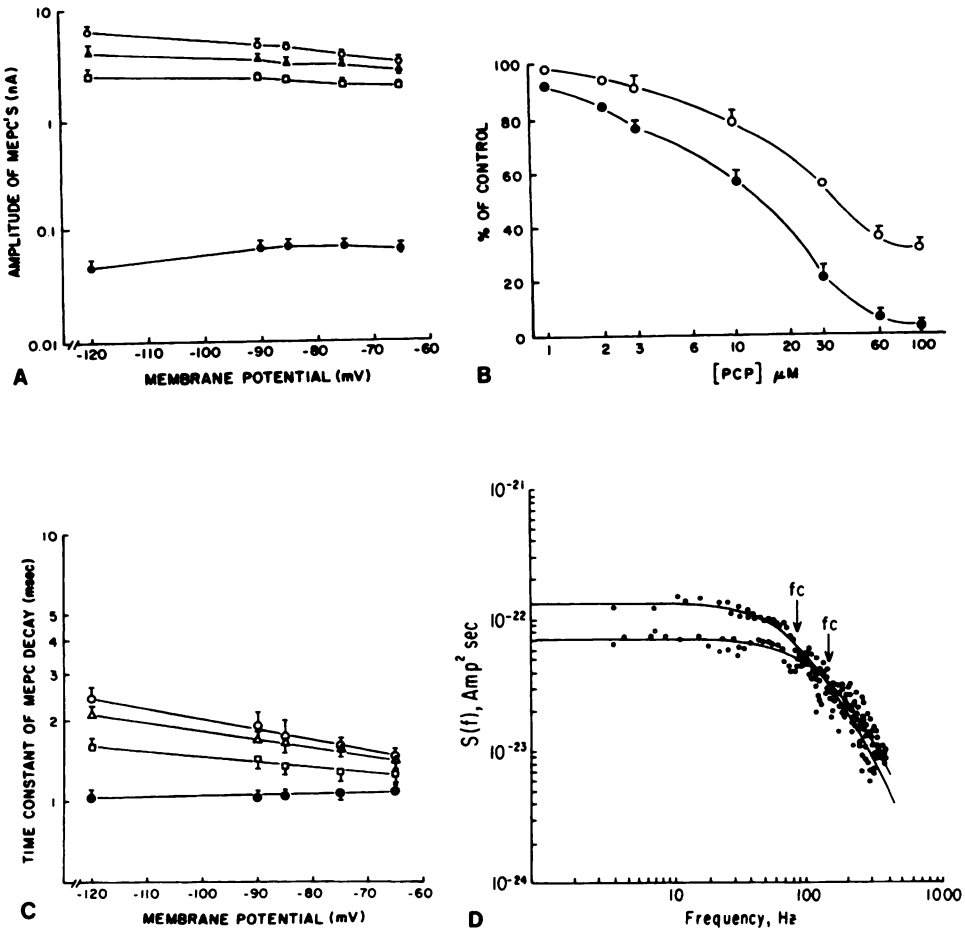

FIG. 8. *Effect of PCP on the amplitude and the time constant of the spontaneous MEPC decay recorded at the junctional region of the frog sartorius muscles*

(A) Plots of current–voltage relationship of the MEPC peak amplitude. (B) Dose–response relationship accompanying the effect of PCP on the peak amplitude and time constant of MEPC decay. The depression of the amplitude (●) during exposure to PCP was more marked than the shortening of the decay time constant (○). (C) Semilogarithmic plots of the relationship between time constant of MEPC decay and membrane potential. Panels A and C show control condition (○) and after 15–120 min of exposure to PCP at concentrations of 3 μM (△), 10 μM (□), and 30 μM (●). (D) Power spectrum of the spontaneous MEPC contained in groups of 512 points sampled at 2 kHz. The points shown are the averages of the MEPC spectrum after subtraction of an averaged baseline spectrum, i.e., without MEPCs. The solid line is the Lorentzian line of the best fit. Each arrow shows the half-power frequency (fc) which is 83 Hz for control (●), giving a channel lifetime (τ) of 1.91 ms, and is 138 Hz during exposure to PCP (3 μM) (○), giving a τ of 1.15 ms (fc = 138 Hz). The holding membrane potential was −80 mV and a sample of 100 MEPCs recorded from three different functional regions. Temperature was 23°C.

reciprocal plots of [^{3}H]H_{12}-HTX binding to the ionic channel in the absence and presence of two concentrations of PCP are shown in Fig. 11. Within the error of the binding determinations, the Y intercepts were not different, suggesting a competitive inhibition. More conclusive evidence for this is presented in the inset to Fig. 11, where the slopes of the double-reciprocal binding curve lines are plotted as a function of PCP concentration. The straight line indicates a competitive inhibition in which PCP and [^{3}H]H_{12}-HTX binding is mutually exclusive. Linear regression analysis of line parameters indicates a K_i of 6.9 μM.

The ability of PCP to inhibit [^{3}H]H_{12}-HTX binding was enhanced two- to sixfold by the inclusion of 10 μM carbamylcholine in the incubation medium (Fig. 10). [^{3}H]H_{12}-HTX (2 nM) binding was increased up to 95% by carbamylcholine (Fig. 12). The concentration of carbamylcholine giving half of maximal stimulation was 60 nM. This increase appeared to represent an increased [^{3}H]H_{12}-HTX affinity rather than an increase in the number of HTX binding sites since maximal binding was unchanged at ion-channel-saturating concentrations of [^{3}H]H_{12}-HTX (5–8 μM). [^{3}H]H_{12}-HTX binding in the presence of 3.2 μM PCP showed a biphasic pattern. Binding was potentiated at carbamylcholine concentrations from 10 to 300 nM (although to a somewhat lesser extent than in the absence of PCP) and inhibited at higher concentrations. Apparently the binding of both H_{12}-HTX and PCP to the ion channel is potentiated by the presence of carbamylcholine, although the effect on PCP is greater than that on H_{12}-HTX.

Data from more detailed analyses of PCP binding to the ion channel in the absence and presence of 10 μM carbamylcholine are presented (Fig. 13 and Table 4). Scatchard plots of PCP binding were linear, and the K_d was calculated to be 10.3 ± 4.2 μM for PCP in the absence of carbamylcholine (Fig. 13). The K_d value was reduced to 2.0 ± 1.3 μM for PCP in the presence of 10 μM

TABLE 3

Effect of various concentrations of PCP on single channel conductance (γ) and channel lifetime (τ_{MEPC}, τ_1) in the frog endplate at −80 mV[a]

Condition	γ (pS)	τ_{MEPC} (ms)	τ_1 (ms)
Control	22.6 ± 0.3	2.20 ± 0.09	1.59 ± 0.03
PCP (0.5 μM)	23.3 ± 0.6	2.10 ± 0.08	1.53 ± 0.03
PCP (1 μM)	21.9 ± 0.5	1.80 ± 0.05	1.45 ± 0.08[b]
PCP (3 μM)	22.4 ± 0.4	1.28 ± 0.07[b]	1.25 ± 0.06[c]
PCP (10 μM)	—	1.14 ± 0.03[b]	—
PCP (30 μM)	—	0.78 ± 0.02[b]	—

[a] Data obtained after 15–20 min exposure to PCP. Each value represents a mean ± SEM of 10 different spectra obtained from five endplates of three sartorius muscles.

[b] $P < 0.05$.

[c] $P < 0.01$.

carbamylcholine. The Hill plot of PCP binding was linear, and the Hill coefficient was 1.0 ± 0.2, and it was unaffected by the presence of carbamylcholine (Table 4).

DISCUSSION

The results of the present investigation demonstrate that PCP reacts with the ionic channel of the nicotinic ACh receptor, thus supporting our initial observation (4). The voltage-dependent inhibition by PCP of EPC amplitude (Fig. 1) and the marked nonlinearity of the current–voltage relationship are quite similar to those seen with other agents that interact with the ionic channel such as atropine and scopolamine (22), HTX and its analogs (15, 16, 23), amantadine (10), and tetraethylammonium (13). The acceleration of the time constant of decay of the EPC and MEPC caused by PCP (Fig. 7, Table 1), the shortening of the mean lifetime of the single ionic channel (Figs. 8, 9, Table 3), and the competition

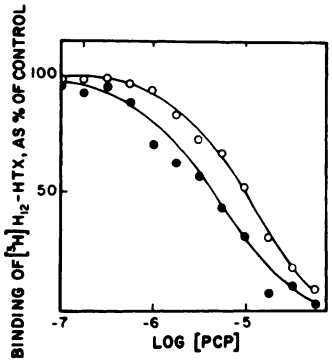

FIG. 10. *Effect of PCP on the specific [³H]H_{12}-HTX (2 nM) binding to the sites of the ionic channel of the ACh receptor in Torpedo membranes in the presence (●) and absence (○) of 10 μM carbamylcholine, plotted as a function of the concentration of PCP (in M)*

with the H_{12}-HTX binding sites (Figs. 10 and 11) strongly suggest a direct action of PCP on the ionic channel of the ACh receptor. Further, the effects of PCP on the ionic channel appear to occur as the result of a reaction of PCP with sites located in the outer and inner surfaces of the ionic channel. The latter conclusion is suggested by our finding that PCP methiodide, which, unlike PCP, does not cross the membrane and is unable to block K^+ conductance when applied in the bath. However applied outside or injected inside the cell it produces depression of the peak amplitude and acceleration of the decay time constant of EPC (unpublished results).

Reaction of PCP with the closed and open conformation of the ionic channel. The effect of PCP on the current–voltage relationship is similar to that seen with tetraethylammonium (13). It involves an initial linear segment followed by nonlinearity and a subsequent neg-

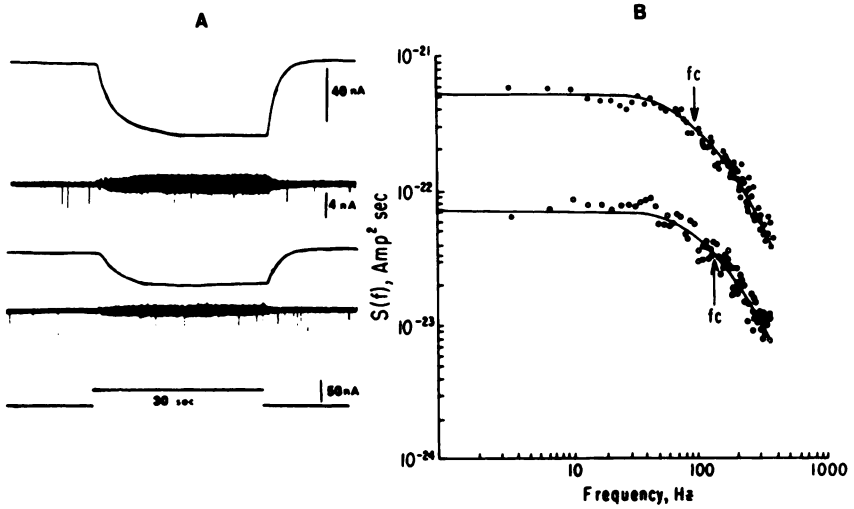

FIG. 9. *Effect of PCP (3 μM) on the voltage-clamped ACh-induced EPCs and MEPCs of the frog sartorius muscles*

The upper records (low gain, dc coupled) on A show the EPC produced by iontophoresis of ACh and the lower traces (high gain, ac coupled) illustrate the fluctuations of currents with spontaneous MEPC. The bottom trace shows the iontophoretic current which was identical for control and for PCP. PCP significantly depressed the EPC induced by iontophoresis of ACh. (B) Power spectra of ACh-induced current fluctuations obtained before (●) and after (○) exposure to PCP for 15 min. The lines are the least-squares fit of the points of a single Lorentzian line. The half-power frequency (*fc*) is indicated by arrows, and was 103 Hz in control and 128 Hz in the presence of PCP. Single-channel conductance and lifetime were 22.8 pS and 1.54 ms in control and 22.2 pS and 1.24 ms in the presence of PCP. The holding membrane potential was −80 mV and the temperature 23°C.

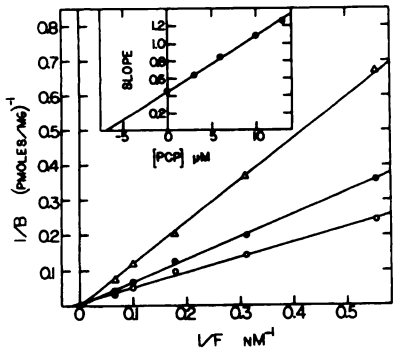

FIG. 11. *Double-reciprocal plots of [^{3}H]H_{12}-HTX binding in the presence of PCP*

[^{3}H]H_{12}-HTX binding (1.8–15 μM) was measured in the presence of 0 (○), 3 (●), and 13 (△) μM PCP. All lines are drawn from linear regression analyses. *B* is pmol [^{3}H]H_{12}-HTX bound per mg protein; *F* is free concentration of [^{3}H]H_{12}-HTX in nM. The inset shows the slopes of these lines, as well as those for binding curves performed in the presence of 6 and 10 μM PCP, plotted as a function of PCP concentration according to the relationship: slope = $(K_d/B_{max}K_i)(I) + K_d/B_{max}$, where K_d and B_{max} are the dissociation constant and total concentration of binding sites for [^{3}H]H_{12}-HTX, respectively, K_i is the inhibition constant, and *I* is the concentration of the inhibitor (i.e., PCP). The *X* intercept (=$-K_i$) is −6.9 μM.

ative conductance. However, qualitatively similar to HTX (15, 16) and unlike tetraethylammonium (13), the nonlinearity and voltage-pathway sensitivity of the EPC observed in the presence of PCP appear to occur as a result of interaction of PCP with a site that is sensitive to the potential field across the junctional membrane. Indeed, this voltage-pathway sensitivity seen in several of the endplates studied with PCP is abolished when conditioning pulses are shortened from 3 s to 25 ms (Fig. 3B).

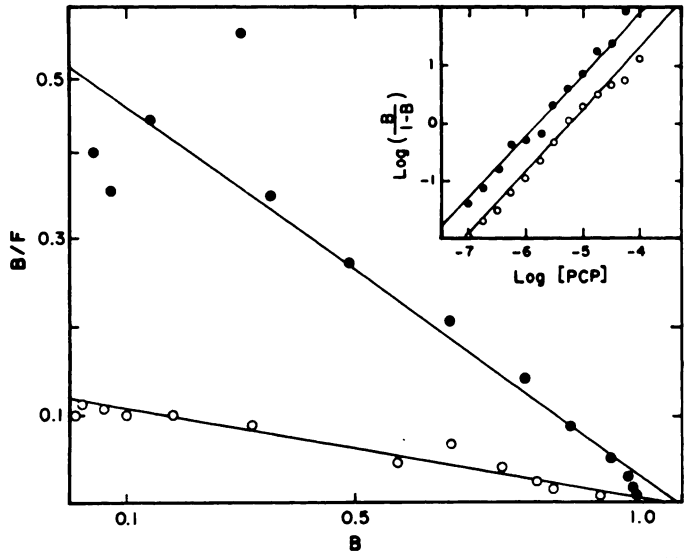

FIG. 13. *Binding of PCP to the sites of the ionic channel of the ACh receptor in Torpedo membranes*

Scatchard and Hill plots (inset) for the binding of PCP to the ion channel sites in the presence (●) and absence (○) of 10 μM carbamylcholine. PCP binding is inferred from the inhibition of specific [^{3}H]H_{12}-HTX binding. Lines are drawn from linear regression analyses. The data are from duplicate experiments; binding parameters from several experiments are summarized in Table 3. The dissociation constants for PCP binding are 11.7 and 2.2 μM in the absence and presence of carbamylcholine, respectively, and the Hill coefficients are 1.10 and 1.07 in the illustrated experiments. *B* is PCP bound as fraction of total binding; *F* is free PCP concentration in μM.

The effect of PCP on the peak amplitude of the EPC does not appear to be dependent upon previous activation of the ACh receptor, i.e., a similar depression of the EPC is observed immediately after the conditioning pulse

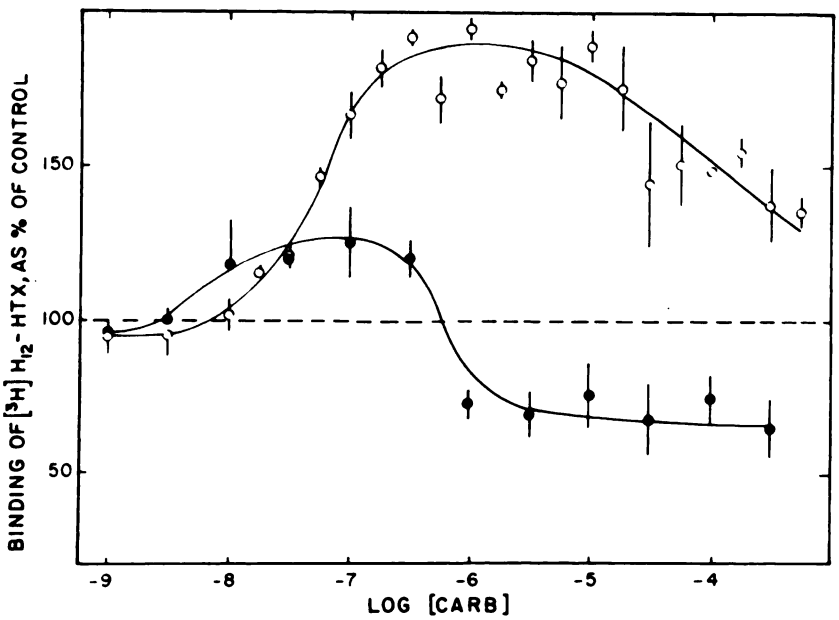

FIG. 12. *Influence of carbamylcholine on [^{3}H]H_{12}-HTX binding to the sites of the ionic channel of the ACh-receptor in Torpedo membranes and on the ability of PCP to inhibit this binding*

The binding of 2 nM [^{3}H]H_{12}-HTX in the absence (○) and presence (●) of 3.2 μM PCP (expressed as percentage of HTX binding in the absence of carbamylcholine and PCP) was measured after 30 min incubation and is plotted as a function of carbamylcholine concentration (in M). The data points and bars represent the means and standard deviations from three independent determinations.

TABLE 4

Dissociation constants (K_d) and Hill coefficients (n) for PCP binding to the nicotinic ionic channels in Torpedo ocellata in the absence and presence of 10 μM carbamylcholine

Values listed represent the mean ± SEM for the indicated number of samples (*N*).

Ligand	K_d	*n*	*N*
PCP	10.3 ± 4.2	1.01 ± 0.15	7
PCP + carbamylcholine	2.0 ± 1.3	1.05 ± 0.24	5

being generated whether or not during the hyperpolarizing step activation of the receptor has occurred. The action of PCP on the current–voltage relationship requires several milliseconds to equilibrate. This time of equilibration is qualitatively equivalent to that seen for HTX and analogs (15, 16, 23) and piperocaine (12), thus indicating that in many cases studied the nonlinearity produced by PCP is dependent upon the duration of the conditioning pulse used (Figs. 3 and 4). Under this condition the voltage- and time-dependent effect that occurs in the hyperpolarized junctional membrane even before the activation of the ACh receptor suggests that PCP may induce this effect by initially reacting with the channel in its resting (closed) conformation. The nonlinearity observed and the current–voltage relationship with PCP is much more pronounced than that seen with atropine and scopolamine (22).

The effect of PCP on τ is detected with concentrations as low as 1 μM. The shortening of τ increases as the concentration of PCP is raised up to a maximal concentration of 100 μM. At 100 μM the time constant of decay becomes as short as 0.5 ms. This shortening of τ with PCP (see Fig. 6) is in sharp contrast to that seen with HTX. At a concentration of HTX of 20 μM the τ_{epc} at −90 to −150 mV is reduced to approximately 1 ms. Concentrations higher than this decrease the EPP amplitude further to the point where no recordings of EPC can be made but without reducing τ_{epc} below 1 ms (unpublished results). These findings suggest that the actions of HTX and PCP share some similarities, but there are differences in their specific binding sites on the ionic channel.

The endplate channel is believed to exist in open and closed conformations (24–27). Since PCP binds to the ionic channel in the absence of ACh (see Fig. 10) it is possible that the voltage-dependent depression of the EPC peak amplitude caused by the agent could result from a voltage-dependent blockade of the closed channel. This conclusion is further supported by the finding that the depression of the EPC in the presence of HTX or PCP does not require prior activation of the ACh receptor (15). Further, an important indication that PCP is reacting with the channel at the closed as well as the open conformation is revealed in Figs. 7 and 8B, where the percentage reduction in EPC peak amplitude was much more than in τ_{EPC} with every PCP concentration tested (Fig. 7). The explanation for this preferential action of PCP on the peak amplitudes of the current vs their decay times could be related to the ability of the agent to block the endplate channel in closed conformation in contrast to its action on the decay time which arises from the blockade of the channel in open conformation, both reactions being voltage sensitive. The blockade of the channel in open conformation causing depression of the EPC amplitude is similar to that seen with atropine (23, 28, 29). In order for the marked nonlinearity seen with PCP to be explained by blockade of the open channel, τ_{EPC} or τ_{MEPC} would have to become much shorter with hyperpolarization over the range of PCP concentrations used. Thus, one has to postulate that PCP binds to both open and closed conformations of the endplate channel.

Effect of PCP on the kinetics of the ACh receptor–ionic channel complex. The assumption that PCP acts on both the open and closed conformations of the channel can be tested using kinetic models and computer simulations of the EPC. According to theoretical considerations, the maximum depression in the EPC peak amplitude at the shortest τ observed (0.5 ms) would be 50% (22), whereas the actual depression is 94%. In previous studies we have shown that a sequential model in which the drug molecule is assumed to bind to the endplate channel after it is opened by ACh can account for both the alteration in τ and the curvature produced in the current–voltage relationship by agents such as atropine and scopolamine (22). Since the abbreviation of the channel lifetime follows blockade of the open channel (18, 23, 31) this would lead to a shortening in the EPC decay and a corresponding decrease in the peak EPC amplitude. Since both events depend on a single perturbation, it is clear that changes in peak EPC amplitude and τ will have similar concentration and voltage dependence, as observed experimentally (22). Indeed, the acceleration of the EPC or MEPC decay without change in their exponential nature suggests that the conductance of the blocked channel is rather low or near zero and that the dissociation of the drug from the channel is also relatively slow (22, 30–32). The sequential model that represents the actions of atropine (22) does not account for the action of PCP because, as mentioned previously, there is a difference in the concentration and voltage dependence of the effect of the agent on the EPC amplitude and the channel lifetime (Figs. 4 and 8B). The reaction of PCP with the closed channel occurs in a manner quite independent of the activation of the receptor as shown by the binding of $[^3H]H_{12}$-HTX to the ionic channel sites in the absence of a cholinergic agonist.

If one postulates that PCP binds to the closed channel without reacting with the ACh receptor itself, it is possible for PCP to alter peak amplitude of the EPC without appreciably affecting τ. Thus, binding of PCP to the closed channel (R) may be responsible for most of the voltage-dependent depression of the peak amplitude, while the binding to the open channel (R*) would be responsible for the shortening and alteration of the voltage dependence of τ. Under this condition, the sequential model has to be modified and extended for PCP by adding a reaction in which PCP combines with R to produce an inactive species (R_D) prior to receptor activation. We used a similar model to explain the synaptic effects of tetraethylammonium (13). However, in contrast, several difficulties were encountered. For example, simulations using the model described below did not

predict as nearly complete a saturation in the relationship between τ_{EPC} and membrane potential as observed experimentally with tetraethylammonium. In fact, it predicted closely the concentration-dependent effect of PCP on τ. Further, tetraethylammonium decreased γ, an effect not seen with PCP (Fig. 6). Thus the hybrid model written below accurately predicts not only the nonlinearities and looping in the current–voltage relationship, but also a rather complex alteration in the rise and decay constants of the EPC and MEPC.

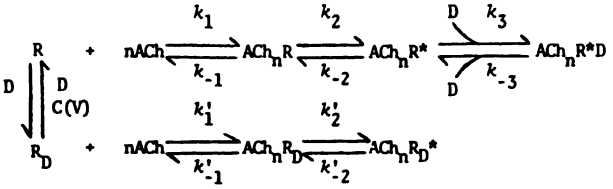

R represents the resting conformation of the receptor–channel complex; n, the number of ACh molecules (1 or 2) that combine with one receptor molecule to cause opening of an ionic channel; ACh_nR and ACh_nR^*, the closed and open conformations of the activated receptor–channel complex, respectively; ACh_nR^*D, the open channel blocked by drug molecule (D) and devoid of conductance. We have assumed that 1 or 2 (n) molecules of ACh combine with R, that the rate constants for ACh binding (k_1) and dissociation (k_{-1}) are voltage dependent (22), and that the rate constants mediating the opening (k_2) and closing (k_{-2}) of channels depend exponentially on membrane potential (22). There is transient formation of a nonconducting state of the channel mediated by the voltage-dependent rate constants k_3 and k_{-3}. $C(V)$ is the voltage-dependent equilibrium dissociation constant regulating the distribution of receptors between R and R_D. Binding by ACh to R_D produces a parallel branch which ultimately leads to a species with little or no conductance ($ACh_nR_D^*$). The rate constants for the ACh binding and dissociation reactions (k_1' and k_{-1}'), and subsequent conformational changes (k_2' and k_{-2}') are assumed to be identical to their normal counterparts. This model was then tested experimentally (unpublished results), and the initial results disclose a reliable fitting between experimental data and simulated data. Thus, the results indicate that with suitable changes of rate constants and parameters the model can account for the alteration of EPC, MEPC, and elementary events involving the concentration dependence of both τ and the peak EPC amplitude, the nonlinearity, and also the time-dependent effect. The model, however, does not explain the differential effect of PCP, and further investigation of the mechanism for this action is required.

In summary, the effect of PCP does not involve the ACh receptor per se, but at least two binding sites at the ionic channel, one located on the channel in its open conformation and the other in its closed conformation. The time-dependent effect is independent of ACh binding to the receptor, but the blockade of the open channel requires marked activation by the reaction of ACh with the receptor.

ACKNOWLEDGMENTS

We are grateful to Dr. John Daly of the National Institutes of Health for kindly providing us with labeled and unlabeled perhydrohistrionicotoxin and to Ms. Mabel Alice Zelle for the computer analyses.

REFERENCES

1. Maayani, S., H. Weinstein, N. Ben-Zvi, S. Cohen and M. Sokolovsky. Psychotomimetics as anticholinergic agents. I. 1-Cyclohexylpiperidine derivatives:: anticholinesterase activity and antagonist activity to acetylcholine. *Biochem. Pharmacol.* **23:** 1263–1281 (1974).
2. Paster, Q., S. Maayani, H. Weinstein and M. Sokolovsky. Cholinolytic action of phencyclidine derivatives. *Eur. J. Pharmacol.* **25:** 270–274 (1974).
3. Weinstein, H., S. Maayani, S. Srebrenik, S. Cohen and M. Sokolovsky. Psychomimetic drugs as anticholinergic agents. II. Quantum mechanical study of molecular interaction potentials of cyclohexylpiperidine derivatives with the cholinergic receptor. *Mol. Pharmacol.* **9:** 820–834 (1973).
4. Tsai, M.-C., R. S. Aronstam, M. E. Eldefrawi, A. T. Eldefrawi and E. X. Albuquerque. Phencyclidine interaction with the nicotinic acetylcholine receptor ionic channel complex and effect on potassium conductance. *Fed. Proc.* **38:** 274 (1979).
5. Kloog, Y., A. Gabrielalevitz, A. Kalir, D. Balderman and M. Sokolovsky. Functional evidence for a second binding site of nicotinic antagonists using phencyclidine derivatives. *Biochem. Pharmacol.* **28:** 1447–1450 (1979).
6. Changeux, J.-P., M. Kasai and C.-Y. Lee. Use of a snake venom toxin to characterize the cholinergic receptor protein. *Proc. Natl. Acad. Sci. USA* **67:** 1241–1247 (1970).
7. Eldefrawi, A. T., N. M. Bakry, M. E. Eldefrawi, M.-C. Tsai and E. X. Albuquerque. Nereistoxin interaction with the acetylcholine receptor ionic channel complex. *Mol. Pharmacol.* **17:** 172–179 (1980).
8. Albuquerque, E. X., E. A. Barnard, T. H. Chiu, A. J. Lapa, J. O. Dolly, S.-E. Jansson, J. Daly and B. Witkop. Acetylcholine receptor and ion conductance modulator sites at the murine neuromuscular junction: evidence from specific toxin reactions. *Proc. Natl. Acad. Sci. USA* **70:** 940–953 (1973).
9. Eldefrawi, A. T., M. E. Eldefrawi, E. X. Albuquerque, A. C. Oliveira, N. Mansour, M. Adler, J. W. Daly, G. B. Brown, W. Burgermeister and B. Witkop. Perhydrohistrionicotoxin: a potential ligand for the ion conductance modulator of the acetylcholine receptor. *Proc. Natl. Acad. Sci. USA* **74:** 2172–2176 (1977).
10. Tsai, M.-C., N. A. Mansour, A. T. Eldefrawi, M. E. Eldefrawi and E. X. Albuquerque. Mechanism of action of amantadine on neuromuscular transmission. *Mol. Pharmacol.* **14:** 787–803 (1978).
11. Tsai, M.-C., A. C. Oliveira, E. X. Albuquerque, M. E. Eldefrawi and A. T. Eldefrawi. Mode of action of quinacrine on the acetylcholine receptor ionic channel complex. *Mol. Pharmacol.* **16:** 382–392 (1979).
12. Tiedt, T. N., E. X. Albuquerque, N. M. Bakry, M. E. Eldefrawi and A. T. Eldefrawi. Voltage- and time-dependent actions of piperocaine on the ion channel of the acetylcholine receptor. *Mol. Pharmacol.* **16:** 909–921 (1979).
13. Adler, M., H. C. Oliveira, E. X. Albuquerque, N. A. Mansour and A. T. Eldefrawi. Reaction of tetraethylammonium with the open and closed conformations of the acetylcholine receptor ionic channel complex. *J. Gen. Physiol.* **74:** 129–152 (1979).
14. Tsai, M.-C., E. X. Albuquerque, D. J. Triggie, R. S. Aronstam, A. T. Eldefrawi and M. E. Eldefrawi. Sites of action of phencyclidine. I. Effects on the electrical excitability and chemosensitive properties of the neuromuscular junction of skeletal muscle. *Mol. Pharmacol.* **18:** 159–166 (1980).
15. Masukawa, L. M. and E. X. Albuquerque. Voltage- and time-dependent action of histrionicotoxin on the endplate current of the frog muscle. *J. Gen. Physiol.* **72:** 351–367 (1978).
16. Albuquerque, E. X. and A. C. Oliveira. Physiological studies on the ionic channel of nicotinic neuromuscular synapses, in "*Advances in Cytopharmacology*" (B. Ceccarelli and F. Clementi, eds.). Raven Press, New York, Vol. 3, 197–211 (1979).
17. Albuquerque, E. X., K. Kuba and J. Daly. Effect of histrionicotoxin on the ionic conductance modulator of the cholinergic receptor: A quantitative analysis of the endplate current. *J. Pharmacol. Exp. Ther.* **189:** 513–524 (1974).
18. Eldefrawi, M. E., A. T. Eldefrawi, N. A. Mansour, J. W. Daly, B. Witkop and E. X. Albuquerque. Acetylcholine receptor and ionic channel of *Torpedo* electroplax: binding of perhydrohistrionicotoxin to membrane and solubilized preparations. *Biochemistry* **17:** 5474–5484 (1978).
19. Katz, B. and R. Miledi. The binding of acetylcholine to receptors and its removal from the synaptic cleft. *J. Physiol. (Lond.)* **231:** 549–574 (1973).
20. Colquhoun, D., W. A. Large and H. P. Rang. An analysis of the action of a false transmitter at the neuromuscular junction. *J. Physiol. (Lond.)* **266:** 361–395 (1977).
21. Gage, P. W. and D. V. Helder. Effects of permanent monovalent cations on endplate channels. *J. Physiol. (Lond.)* **288:** 509–528 (1979).
22. Adler, M., E. X. Albuquerque and F. J. Lebeda. Kinetic analysis of endplate currents altered by atropine and scopolamine. *Mol. Pharmacol.* **14:** 514–529 (1978).
23. Oliveira, A. C., E. X. Albuquerque, J. W. Daly, M. E. Eldefrawi and A. T. Eldefrawi. Effects of histrionicotoxin analogs on the ionic channel of the acetylcholine receptor. *Soc. Neurosci. Abstr.* **4:** 372 (1978).
24. del Castillo, J. and B. Katz. A comparison of acetylcholine and stable depolarizing agents. *Proc. Roy. Soc. B (Lond.)* **146:** 362–368 (1957).

25. Magleby, K. L. and C. F. Stevens. The effect of voltage on the time course of end-plate currents. *J. Physiol.* (*Lond.*) **223:** 151–171 (1972).
26. Magleby, K. L. and C. F. Stevens. A quantitative description of end-plate currents. *J. Physiol.* (*Lond.*) **223:** 173–197 (1972).
27. Neher, F. and B. Sakmann. Noise analysis of drug induced voltage clamp currents in denervated frog muscle fibres. *J. Physiol.* (*Lond.*) **258:** 705–730, (1976).
28. Feltz, A., W. A. Large and A. Trautmann. Analysis of atropine action at the frog neuromuscular junction. *J. Physiol.* (*Lond.*) **269:** 109–130 (1977).
29. Katz, B. and R. Miledi. The effect of atropine on acetylcholine action at the neuromuscular junction. *Proc. Roy. Soc.* (*Lond.*) **184:** 221–226 (1973).
30. Neher, E. and Y. H. Steinbach. Local anaesthetics transiently block currents through single acetylcholine-receptor channels. *J. Physiol.* (*Lond.*) **277:** 153–176 (1978).
31. Steinbach, A. B. A kinetic model for the action of xylocaine on receptors for acetylcholine. *J. Gen. Physiol.* **52:** 162–180 (1968).
32. Adams, P. Voltage jump analysis of procaine action at frog end-plate. *J. Physiol.* (*Lond.*) **268:** 291–318 (1977).

Send reprint requests to: Dr. Edson X. Albuquerque, Department of Pharmacology and Experimental Therapeutics, University of Maryland School of Medicine, Baltimore, Md. 21201.